Thermodynamically-consistent semi-classical -changing rates

2017 J. Phys. B: At. Mol. Opt. Phys. 50 115201

(http://iopscience.iop.org/0953-4075/50/11/115201)

IOP Publishing Journal of Physics B: Atomic, Molecular and Optical Physics
J. Phys. B: At. Mol. Opt. Phys. **50** (2017) 115201 (9pp) https://doi.org/10.1088/1361-6455/aa6f58

Thermodynamically-consistent semi-classical ℓ-changing rates

R J R Williams[1,5], F Guzmán[2], N R Badnell[3], P A M van Hoof[4], M Chatzikos[2] and G J Ferland[2]

[1] AWE plc, Aldermaston, Reading RG7 4PR, United Kingdom
[2] Department of Physics and Astronomy, University of Kentucky, Lexington, KY 40506, United States of America
[3] Department of Physics, University of Strathclyde, Glasgow G4 0NG, United Kingdom
[4] Royal Observatory of Belgium, Ringlaan 3, B-1180 Brussels, Belgium

E-mail: robin.williams@awe.co.uk

Received 17 February 2017, revised 7 April 2017
Accepted for publication 25 April 2017
Published 11 May 2017

Abstract

We compare the results of the semi-classical (SC) and quantum-mechanical (QM) formalisms for angular-momentum changing transitions in Rydberg atom collisions given in a series of papers by Vrinceanu *et al*, most recently Vrinceanu *et al* (2012 *Astrophys. J.* **747** 56), with those of the SC formalism using a modified Monte Carlo realization. We find that this revised SC formalism agrees well with the QM results. This provides further evidence that the rates derived from the QM treatment are appropriate to be used when modeling recombination through Rydberg cascades, an important process in understanding the state of material in the early universe. The rates for $\Delta\ell = \pm 1$ derived from the QM formalism diverge when integrated to sufficiently large impact parameter, b. Further to the empirical limits to the b integration suggested by Pengelly and Seaton (1964 *Mon. Not. R. Astron. Soc.* **127** 165), we suggest that the fundamental issue causing this divergence in the theory is that it does not fully cater for the finite time taken for such distant collisions to complete.

Keywords: Rydberg states, atomic collisions, semi-classical approximations

(Some figures may appear in colour only in the online journal)

1. Introduction

There has been significant recent interest in the rates for angular momentum changing collisions of low velocity ions with Rydberg atoms. While this may seem a somewhat obscure corner of atomic physics, the time to pass through the ladder of high-angular momentum levels in highly excited atoms proves to be a bottleneck in the process of atomic (re-) combination in the early universe. The details of the ℓ-changing rates therefore have a major impact on our understanding of this important stage in cosmic development [1].

For this Stark mixing process to be the dominant, the impact parameter of the collision must be sufficiently large that both the orbital quantum number within the target does not change, and the field due to the collider ion must remain smaller than that of the host nucleus throughout the interaction [2].

The atomic physics of these rates can be calculated by a variety of approximations, developing from classical orbit [3–5] to quantum orbit theory [2, 6–10]. In what follows we will refer to [2, 10] as VF01 and VOS12, respectively. In this paper, we will concentrate on the differences between the most detailed of these formulations, those based on treating the response of the target orbital using quantum-mechanical perturbation theory (QM) and a semi-classical (SC) approach which makes use of classical trajectory theory. As discussed elsewhere ([11, 12], and references therein), these theories result in predictions for integrated rates which differ by up to an order of magnitude, sufficient to have a major impact on the interpretation of observations. This difference is primarily the result of the different range in impact parameter over which $|\Delta\ell| = 1$ transitions are active in the different theories:

[5] Author to whom any correspondence should be addressed.

the QM theory has a logarithmic divergence in transition rate, which requires a limit to be placed on the largest impact parameter for which collisions are active in causing transitions, while in the SC approach as applied by VF01/VOS12, this limit arises as a result of the finite domain in impact parameter over which a single collision can cause a complete $|\Delta\ell| = 1$ transition.

In this paper, we will present the results of calculations using the SC theory of VF01, but using Monte Carlo trajectory binning [6, 13]. We find that with this alternative approach, the SC results agree well with those of the quantum theory. So far as there are differences, these are as would be expected when relating a quantum theory to its classical limit, and are consistent with the correspondence principle. When integrated over impact parameter, b, and a thermal spectrum of colliders, it is clear that the differences in rates computed using this modified SC approach and the original QM formalism will be minimal.

In section 2 we present the background theory, and in section 3 compare the QM transition probabilities with SC probabilities as calculated by VF01 and VOS12, and with our revised approach. In section 4, we briefly discuss how the discretely sampled VF01 SC approach can be made somewhat more accurate, and consistent with the discrete detailed balance relations. Finally, in section 5, we summarize our results, and discuss the processes which prevent the overall dipole transition rate from diverging in a plasma of finite density.

2. Theory

VF01 and VOS12 provide detailed formulae for the rates of transitions $\ell \to \ell'$ for precise values of ℓ, ℓ'. They derive their SC formulae using approximations which correspond to the continuum limit n, ℓ, $\ell' \to \infty$, with ℓ/n and ℓ'/n finite, and then apply them in the case of finite quantum numbers. They apply what they term as a microcanonical ensemble, sampling the fundamentally continuous classical-limit expressions at discrete values of incoming and outgoing angular momentum appropriate for the angular momentum quantum number. Using this procedure provides values for the overall collision rate which are finite for all $\Delta\ell$, as noted above.

The process of returning from the continuum to the discrete limit is not, however, unique. In the present paper, we use a method similar to that discussed by [13]. To ensure thermodynamic consistency for the derived total rates, it is better to follow a finite-volume formalism (see, e.g., [14]), where each of the discrete quantum numbers is taken to correspond to a finite range of continuum values. The simplest assumption which will ensure results are consistent with the thermodynamical equilibrium is to assume that the probability density of states in the continuum band corresponding to each of the aggregate states is internally in thermodynamic equilibrium. As there is no energy difference between states in the case considered by Vrinceanu *et al*, this corresponds to assuming a uniform population. This procedure provides results consistent with the thermodynamic requirements of unitarity and detailed balance and with the quantum and classical limits, as well as with usual practice in Monte Carlo simulation of off-lattice systems [15]. However, it leaves us looking to statistical physics, rather than numerical convention, to understand how to prevent the dipole transition rates from diverging as a result of the long-range nature of the Coulomb interaction.

For the standard quantum mechanical association of the radial quantum number n, the total angular momentum quantum number ℓ satisfies $0 \leqslant \ell \leqslant n - 1$. If we assume that each value of ℓ maps to a shell with total angular momentum between $\ell\hbar$ and $(\ell + 1)\hbar$, with a classical density of states $\propto \ell$ (which may be visualized as a two-dimensional polar coordinate system), then the area of this shell is $\propto 2\ell + 1$. This is consistent with the number of z-angular momentum eigenstates $|m| \leqslant \ell$ corresponding to each total angular momentum eigenstate. It results in a mean-squared angular momentum in the shell of

$$\langle L^2 \rangle = \left[\ell(\ell + 1) + \frac{1}{2}\right]\hbar^2, \tag{1}$$

which is a constant $\hbar^2/2$ greater than the value which enters in quantum mechanical calculations, $\langle L^2 \rangle = \ell(\ell + 1)\hbar^2$. For comparison, assuming that the total angular momentum corresponding to a quantum number ℓ is exactly $\ell\hbar$ underestimates $\langle L^2 \rangle$ by $\ell\hbar^2$, which is a significantly larger error for large ℓ. (Taking the angular momentum for the discrete state to be $\left(\ell + \frac{1}{2}\right)\hbar$ is more accurate, with the classical and quantum density of states being equivalent, and the mean-square angular momentum $\langle L^2 \rangle$ over-estimated by $\hbar^2/4$.)

Transition probabilities in the finite volume regime can be derived from the SC results of VF01/VOS12 by interpreting them as probability density functions in the continuum limit, so the transition probability from the state (n, ℓ) to (n, ℓ') becomes

$$\langle P^{\mathrm{SC}} \rangle_{n\ell\ell'} = \int_{\ell/n}^{(\ell+1)/n} \mathrm{d}\lambda \int_{\ell'/n}^{(\ell'+1)/n} \mathrm{d}\lambda'\, P^{\mathrm{SC}}(\lambda, \lambda', \chi) g(\lambda) g(\lambda') \Big/ \int_{\ell/n}^{(\ell+1)/n} \mathrm{d}\lambda\, g(\lambda), \tag{2}$$

where $g(\lambda) = 2\lambda$ is the classical density of states, normalized so that $\int_0^1 g(\lambda)\mathrm{d}\lambda = 1$, and

$$P^{\mathrm{SC}}(\lambda, \lambda', \chi) = \frac{2\lambda'/n}{\pi\hbar \sin\chi} \begin{cases} 0, & |\sin\chi| < |\sin(\eta_1 - \eta_2)| \\ \frac{K(B/A)}{\sqrt{A}} & |\sin\chi| > |\sin(\eta_1 + \eta_2)| \\ \frac{K(A/B)}{\sqrt{B}} & \text{otherwise,} \end{cases} \tag{3}$$

is the SC transition probability given by VOS12. In this expression, K is the complete elliptic integral,

$$A = \sin^2\chi - \sin^2(\eta_1 - \eta_2), \tag{4}$$

$$B = \sin^2(\eta_1 + \eta_2) - \sin^2(\eta_1 - \eta_2), \tag{5}$$

$$\cos\eta_1 = \lambda, \tag{6}$$

$$\cos\eta_2 = \lambda', \tag{7}$$

and χ is given in terms of n and other implicit parameters of the collision by

$$\cos\chi = \frac{1+\alpha^2\cos\left(\sqrt{1+\alpha^2}\,\Delta\Phi\right)}{1+\alpha^2}, \tag{8}$$

$$\alpha = \frac{3Z_1}{2}\left(\frac{a_n v_n}{bv}\right), \tag{9}$$

where the swept angle $\Delta\Phi$ is assumed to be $-\pi$, and the Stark mixing parameter α depends on the average radius and velocity, a_n and v_n of the target orbital, as well as the charge $Z_1 e$, impact parameter b and velocity v of the impinging ion.

This procedure replaces the closed-form expressions of VF01 and VOS12 with a double integral, so is not as suitable for numerical work. However, it seems worthwhile to compare the results with those of the discrete interpretation in order to inform possible modifications to the VF01/VOS12 formalism which might be made to ensure compatibility with the limit of thermodynamic equilibrium.

There are a number of desirable properties for any set of approximate transition probabilities. These include unitarity, i.e. that the system must reside in one of the angular momentum states at the end of the transition

$$\sum_{\ell'} P_{n\ell\ell'} = 1, \tag{10}$$

and detailed balance, i.e.

$$(2\ell+1)P_{n\ell\ell'} = (2\ell'+1)P_{n\ell'\ell}, \tag{11}$$

for the quantum level degeneracy $g(\ell) = 2\ell + 1$. Note that the sum for the unitarity requirement includes the probability that the scattering leads to no transition, $P_{n\ell\ell'}$ with $\ell' = \ell$. It is possible to determine this rate using the same analytic forms as for the ℓ-changing interactions, and this rate is included in the plots shown below.

The symmetry of the expressions for A and B in λ and λ', together with the overall factor of λ' in equation (3), means that equation (3) satisfies the detailed balance relations *in the continuum limit*,

$$2\lambda P^{\mathrm{SC}}(n,\,\lambda,\,\lambda') = 2\lambda' P^{\mathrm{SC}}(n,\,\lambda',\,\lambda), \tag{12}$$

given the classical density of states $g(\lambda) = 2\lambda$. As a result of this, it is simple to verify that the phase-space average, equation (2), satisfies the discrete detailed balance relation

$$(2\ell+1)\langle P^{\mathrm{SC}}\rangle_{n\ell\ell'} = (2\ell'+1)\langle P^{\mathrm{SC}}\rangle_{n\ell'\ell}. \tag{13}$$

Beyond these absolute requirements, we also suggest that the rates should be subject to another statistical requirement for collisions at small impact parameter. For these scatterings, the output state of the interaction is dependent on complex interference phenomena, sensitive to many details of the atomic physics. However, the net effect of this complexity, when averaged over some small range of incoming particle properties, would be expected to be asymptotically close to the output states being in statistical equilibrium (see, for the classical case, [16]). We therefore suggest that, in the limit of close scatterings $b \to 0$, the rates should be subject to an ergodicity property

$$\langle P\rangle_{n\ell\ell'} \simeq \frac{2\ell'+1}{n^2}, \tag{14}$$

i.e. when the collider passes close enough to the core of the target atom, in the Stark adiabatic region, the effect of the collision is to randomize the output state, when the input state is coarse-grained over a suitable domain. Of course, in reality scatterings will cease to be purely ℓ-changing in this limit. Even so, it is to be expected that the output state angular momentum will become statistically independent within the shell. This requirement seems to be the best physical interpretation which can be put on the statement in [17], hereafter PS64, that in the core the scattering probability becomes a rapidly oscillating function with mean value $\frac{1}{2}$. This is what would result from the core ergodicity principle in the case of a two-level system, so the core ergodicity principle seems like a reasonable generalization, agreeing with the work of PS64 at least in spirit. As we will see, it is also a reasonable description of what in fact happens when the quantum and shell-averaged classical transition probabilities are calculated in detail.

3. Results

3.1. Comparison of QM and SC theory for fixed quantum numbers

In figures 1 and 2, we compare the quantum mechanical probability distributions with the SC transition probabilities sampled at specific ℓ, ℓ'. The QM dipole transition rates, $\Delta\ell = \pm 1$ decay slowly as b increases, which is the origin of the divergence of the rate integral for these transitions. The SC transition probabilities show sharp edges where the transitions first become allowed, for all $\Delta\ell$: the transition rates for all $\Delta\ell$ are similar, as there is nothing in the SC formulation which fundamentally distinguished a $|\Delta\ell| = 1$ transition from one with a larger change in angular momentum. There are also internal peaks for many cases, corresponding to orbital resonances. These are used by VOS12 to limit the domain over which $|\Delta\ell| = 1$ transitions are allowed, avoiding the divergence in the integrated transition rate found for the QM dipole transition rate.

It is clear that the SC transition probabilities cannot satisfy unitarity, as where any transition ceases to be allowed, there is no corresponding increase in the others. Indeed, at sufficiently large radii, the probability of no transition, $P_{n\ell\ell}$, increases above unity, which is inconsistent with usual definition of probability. The quantum transition probabilities do satisfy unitarity (note that the curves as plotted are divided by $2\ell' + 1$ to make the ergodicity property at small b more obvious, but this means that this summation property for the probabilities is less obvious as shown).

In figures 3 and 4, we compare the quantum mechanical probability distributions with the SC probability distributions averaged over angular momentum shells. These plots are significantly more alike than those for the comparison

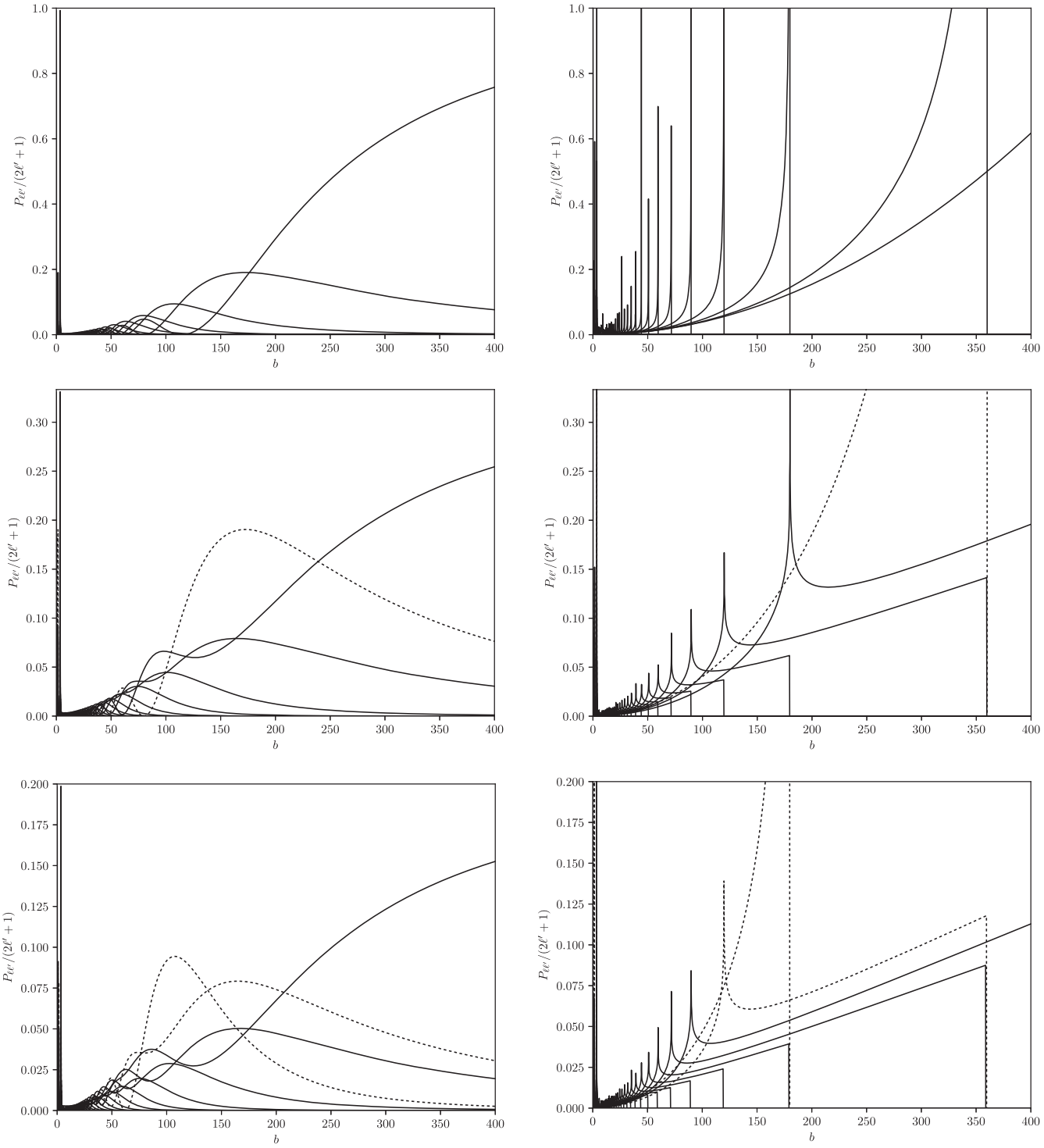

Figure 1. Plots of $P_{n\ell\ell'}/(2\ell'+1)$ versus b for $n = 30$ and $\ell = 0$ (first row), $\ell = 1$ (second row) and $\ell = 2$ (third row). The Stark parameter is $\alpha = 6/b$. Left column is using the QM formalism, right is using the SC formalism. The highest curve at large b has $\Delta\ell = 0$, larger $\Delta\ell$ curves appear in order as b reduces. Dotted curves are for $\ell' < \ell$.

between the quantum mechanical probability and the discretely sampled SC transition probability. While there are no longer any sharp edges in the shell-averaged SC probabilities, for $|\Delta\ell| > 1$ they will be non-zero only within some range of α values. (The integration over a quantized shell width means that there is now a genuine distinction in qualitative behavior between transitions with different $|\Delta\ell|$.) The shell-averaged SC probabilities also satisfy unitarity and the quantum-weighted detailed balance constraint.

Away from the region where the discretely sampled transition probability is zero, the binning has a relatively minor effect, simply smoothing out the steepest peaks.

The general form of the transition probability distributions shown in these figures is of interest. Working from large

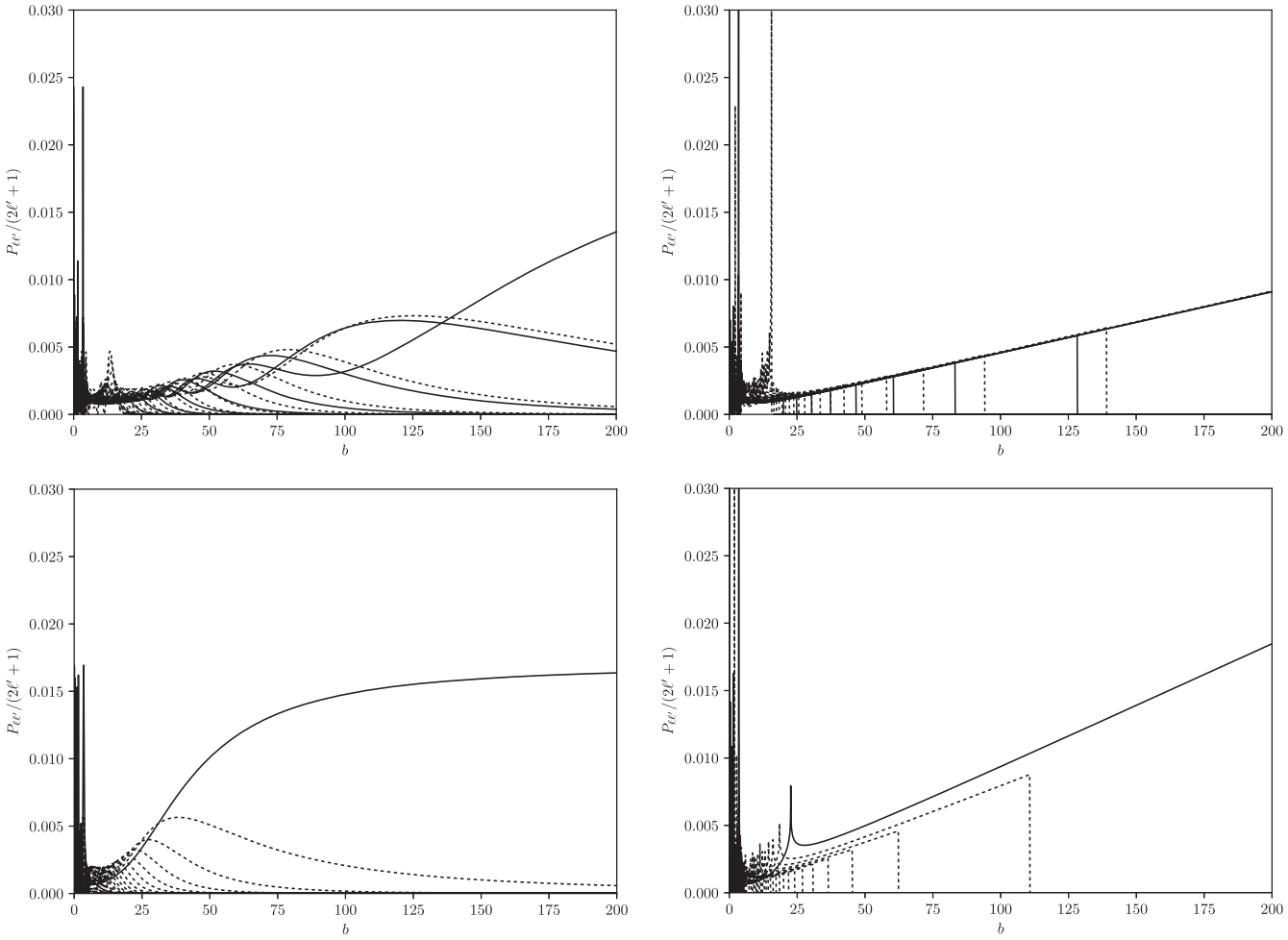

Figure 2. Plots of $P_{n\ell\ell'}/(2\ell' + 1)$ versus b for $\ell = 20$ (first row) and $\ell = 29$ (second row). The n and α parameters are as in figure 1. Left column is using the QM formalism, right is using the SC formalism. Dotted curves are for $\ell' < \ell$. Note that there are no upward transitions for $\ell = 29$ due to the constraint that $\ell' < n$.

b inwards, it is initially most likely that no change in ℓ will result. At least in the QM case, all other values of $\Delta\ell$ are possible, with probabilities reducing as $|\Delta\ell|$ increases. As b becomes smaller, the probabilities of the higher $|\Delta\ell|$ transitions increase, following a smooth power law dependency, until the statisical weight of the output state reaches a similar level to that of the $\Delta\ell = 0$ transition. Thereafter, the probabilities are subject to significant oscillations, around an average level consistent with statistical balance, apart from a strong spike at the very smallest values of b. This suggests that the combination of the asymptotic behavior at large b, the core ergodicity principle, and the fundamental requirements of unitarity and detailed balance, should be sufficient to provide thermodynamically consistent estimates of the impact-parameter and thermal-averaged rates which would be acceptably accurate for many applications.

3.2. The classical limit of the QM formalism

Having shown that the SC results can be made acceptably consistent with those of the QM formalism by an appropriate binning procedure, it is also of interest to demonstrate consistency in the opposite direction. To do this, in figure 5, we compare the non-averaged SC probability for one transition with a series of QM results with quantum numbers increasing by factors of 2. As the quantum numbers increase, while maintaining their ratios, the QM results tend to the SC limit, with the resolution of sharp features, including the orbital resonances seen in the classical results, gradually improving. Oscillations remain within the classically allowed range, and long tails in the classically forbidden range. This combination of Gibbs phenomenon ringing and evanescent tunneling behavior, typical of the Airy function, is characteristic of the classical limit of quantum phenomena. The QM formalism remains accurate for all values of the quantum numbers, but the expressions for the rates become increasingly difficult to evaluate numerically.

4. Use of SC probabilities

The shell-sampled probabilities presented in the previous section are determined using a computationally expensive double integral. It may be possible to perform one or both of

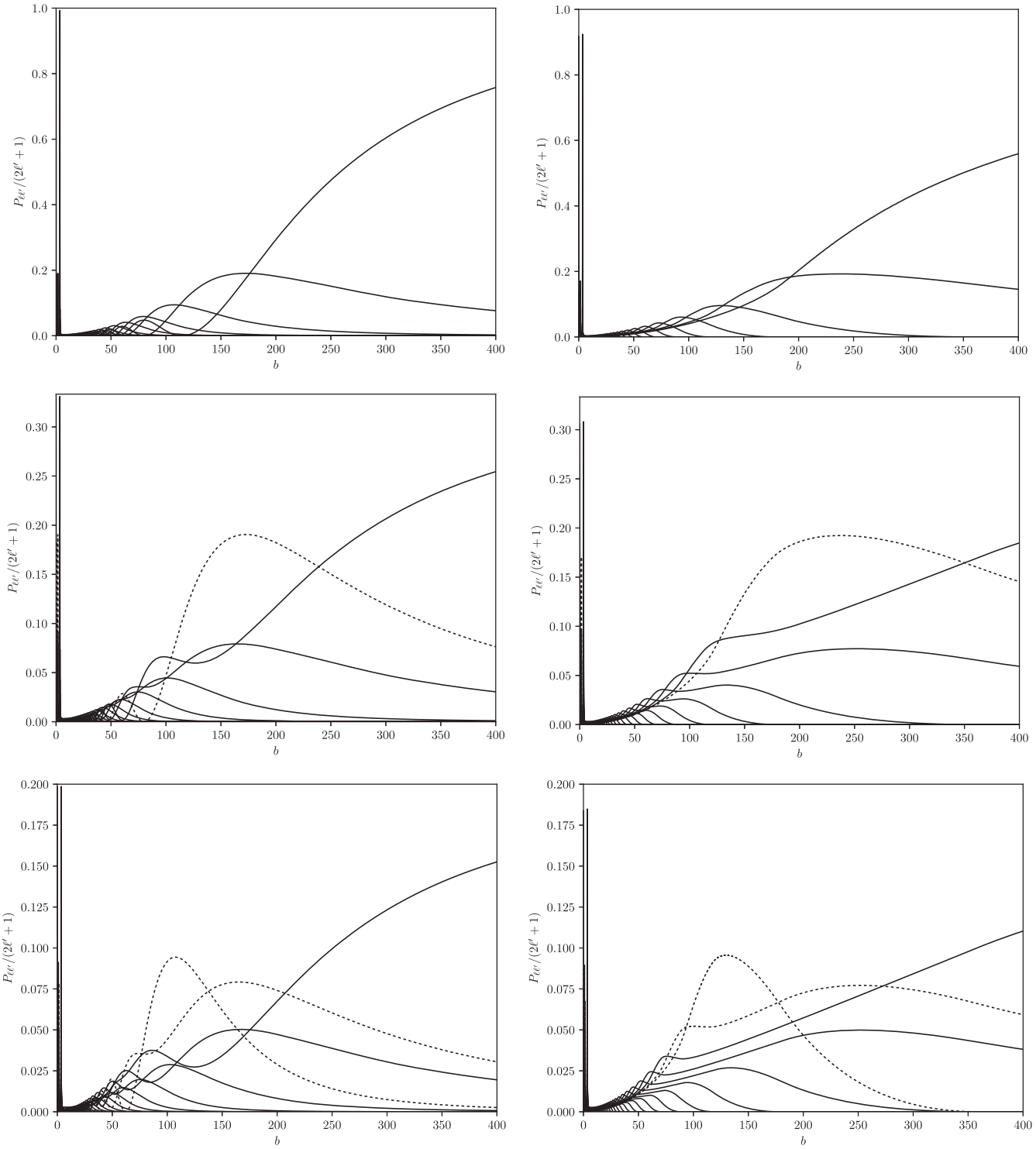

Figure 3. Plots of $P_{n\ell\ell'}/(2\ell'+1)$ versus b for $\ell = 0$ (first row), $\ell = 1$ (second row) and $\ell = 2$ (third row). Left column is using the QM formalism, right is using the SC formalism, averaged over shells. Dotted curves are for $\ell' < \ell$.

these integrals analytically, but numerical results were sufficient for the present analysis.

However, given that the use of a classical transition rate is already a significant approximation, using a point sample of the transition rate rather than an integral is likely to be an acceptable approximation, at least away from the case of $\Delta\ell = \pm 1$, $b \to \infty$. As these rates are being attributed to quantum mechanical rather than classical states, it makes sense to ensure the rates are chosen so as to satisfy quantum mechanical rather than classical statistics. The most consistent identification of quantum mechanical states with a continuum band has $\ell\hbar$ as the angular momentum at the innermost edge of the band. Hence, if a single value based on the classical transition probability is to be used for this

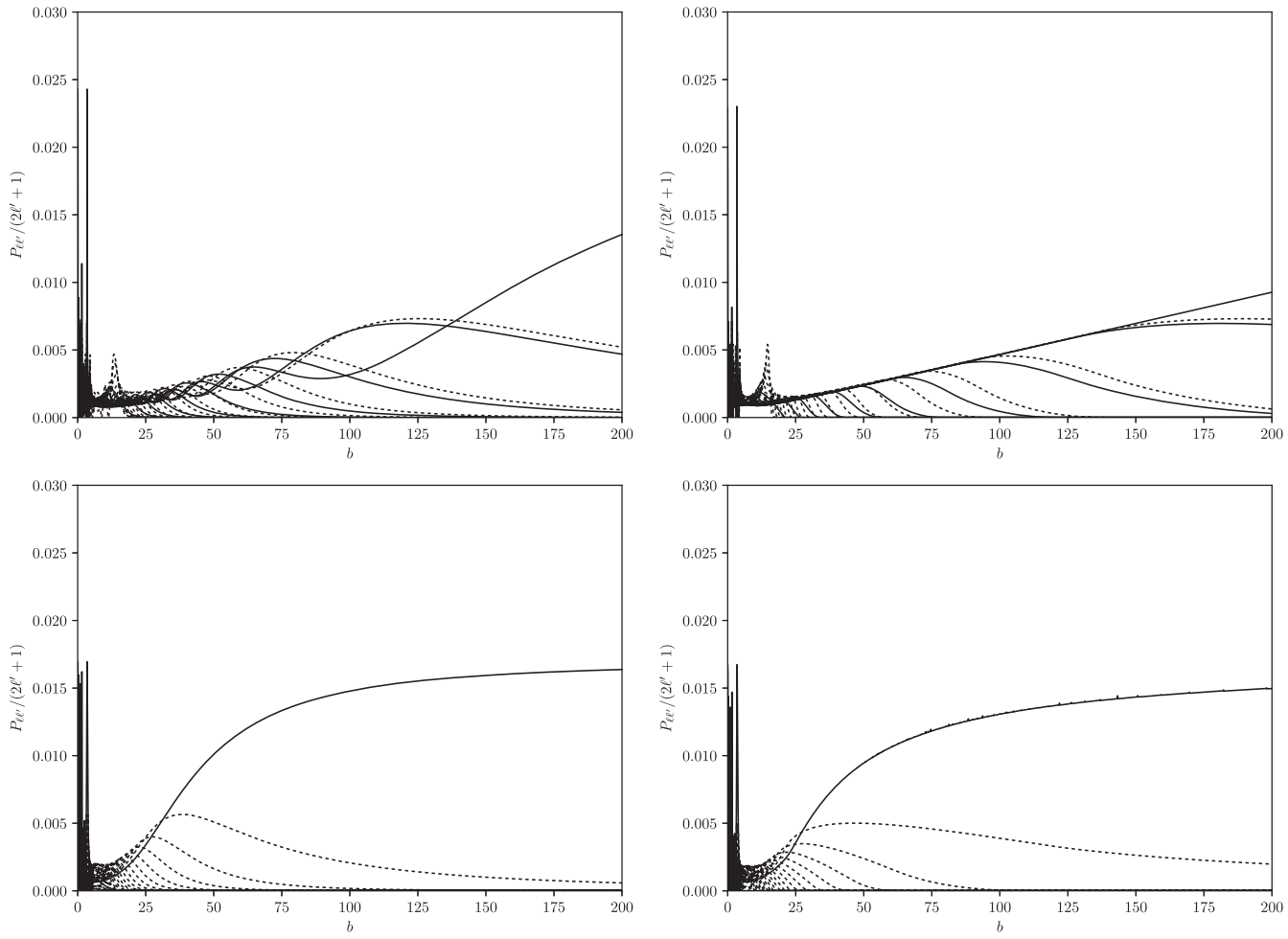

Figure 4. Plots of $P_{n\ell\ell'}/(2\ell'+1)$ versus b for $\ell = 20$ (first row) and $\ell = 29$ (second row). Left column is using the QM formalism, right is using the SC formalism, averaged over shells. Dotted curves are for $\ell' < \ell$.

quantum number, it will be accurate to a higher order if the angular momentum used in this expression is somewhat higher than $\ell\hbar$. In particular, in order to be consistent with the quantum mechanical detailed balance condition, the value $2\ell'+1$ should be used in the numerator of the pre-factor of equation (6) of VOS12. This means that the $\ell \to \ell' = 0$ rates will not be strictly zero, as required by the expressions given by VF01. Given that VF01 provide expressions for the transition rate *out* of an $\ell = 0$ state, a zero inward rate is in clear violation of the detailed balance requirement.

The values used in the elliptic integral terms must be symmetric functions of ℓ, ℓ', as is true for the expressions given. Ideally they should also be chosen to satisfy unitarity, but in reality the correction to the overall transition rates as a result of violating this constraint will be small compared to the other approximations underlying this approach. Using $\cos\eta_1 = \left(\ell + \frac{1}{2}\right)/n$, etc, will be at least somewhat more accurate than without the $\frac{1}{2}$, and also means that the cases $\ell = 0$, $\ell' = 0$ do not require a special treatment.

5. Conclusions

We have shown that, by using an alternative form for the Monte Carlo realization, the results for the SC and QM formalisms described by VF01 and VOS12 can be brought closely into line. As this is consistent with what is expected as a result of the correspondence principle, it provides further evidence that the results of the QM formalism of VF01 and VOS12 is accurate, and should be preferred over their SC formalism in regimes where their results differ significantly.

While finding agreement between the different forms of theory is satisfying, this does not take into account the major reason given by VF01 and VOS12 for preferring their SC results, specifically the need for an outer limit to be imposed on the integration over impact parameters to prevent the total collision rate diverging for $\Delta\ell = \pm 1$ when using the QM theory. This type of divergence is common in other areas of collision rate physics (in particular, the two-body relaxation time, [18, 19]), so is not unexpected. PS64 give expressions for a variety of empirical limits to the range of b over which Stark mixing will be active, due to Debye screening, target atom state radiative lifetimes, and the lifting of degeneracy

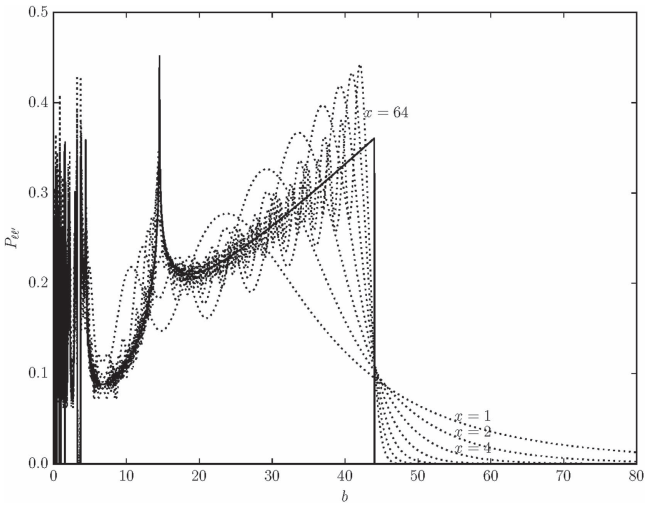

Figure 5. Comparison of the SC $P_{n\ell\ell'}$ versus b for $\ell = 2$, $\ell' = 4$, $n = 8$ transition probability (solid line), compared to a succession of scaled QM formalism probabilities $xP_{n\ell\ell'}$, with $\ell = 2x$, $\ell' = 4x$ and $n = 8x$, where $x = 1, 2, 4, 8, \ldots 64$. As the scaling factor x increases, the QM probabilities tend towards the SC results.

between the ℓ levels as a result of relativistic effects, or the finite core radius for target atoms of species heavier than H. The value of the outer cut-off is taken to be the most constraining of these processes. The logic here is similar to the outer limit applied to the Coulomb logarithm in other contexts, such as two-body relaxation in plasmas. The relevant Debye screening is that which reduces the long-range field of the impinging ion (Debye screening of the charge of the target atom nucleus is in effect a continuum lowering process), and will be rapid for colliders with thermal velocities due to the high mobility of electrons.

Nevertheless, it is also worth noting that as b increases, so does the time over which the collision takes place: the treatment of collisions as independent events must therefore eventually become inaccurate. During the extended period taken to complete the most distant encounters, there will be time for many collisions at smaller impact parameters. While, at first order, the effects of collisions will superpose linearly, at sufficiently large b a limit will be reached where smaller impact parameter collisions together are sufficient to randomize the angular momentum of the target orbital during the time over which the larger b interaction is taking place. Once b increases above the level where this occurs, $b_{\rm eq}$, the effect of collisions at larger impact parameter will be felt, in effect, as a superposition of $N_{\rm coll} \sim \tau_{\rm coll}/\tau_{\rm eq}$ partial interactions adding in quadrature, rather than linearly (where $\tau_{\rm coll}$ is the collision time at the large b of interest, and $\tau_{\rm eq}$ is the collision time at the smallest radius leading to effective randomization). A reduction in contribution to the transition probability by $\sim N_{\rm coll}^{-1/2} \propto b^{-1/2}$ at the largest b will be sufficient to prevent the weak logarithmic divergence in the overall rate. This is a somewhat academic argument, as the plasma particle correlations underlying Debye screening will in general result in more stringent limits to the range of b over which collisions are effective. Nevertheless, given that the agreement we now find between the SC and QM gives greater confidence in SC results for the Rydberg scattering problem, it may be possible to investigate the corrections required for these multiple interactions in a believable manner using explicit classical trajectory calculations.

Acknowledgments

We thank D Vrinceanu and H Sadeghpour for helpful responses to several queries about their published work, and the referees for valuable suggestions. Parts of this work have been supported by the NSF (1108928, 1109061, and 1412155), NASA (10-ATP10-0053, 10-ADAP10-0073, NNX12AH73G, and ATP13-0153), and STScI (HST-AR-13245, GO-12560, HST-GO-12309, GO-13310.002-A, and HST-AR-13914). MC has been supported by STScI (HST-AR-14286.001-A). PvH was funded by the Belgian Science Policy Office under contract no. BR/154/PI/MOLPLAN.

References

[1] Chluba J, Vasil G M and Dursi L J 2010 Recombinations to the Rydberg states of hydrogen and their effect during the cosmological recombination epoch *Mon. Not. R. Astron. Soc.* **407** 599–612

[2] Vrinceanu D and Flannery M R 2001 Classical and quantal collisional Stark mixing at ultralow energies *Phys. Rev.* A **63** 032701

[3] Percival I C and Richards D 1979 Classical theory of transitions between degenerate states of excited hydrogen atoms in plasma *J. Phys. B: At. Mol. Phys.* **12** 2051–65

[4] Kazansky A K and Ostrovsky V N 1995 Classical theory of l-changing transitions in collisions between Rydberg atoms and ions *Phys. Rev.* A **52** R1811–4

[5] Kazansky A K and Ostrovsky V N 1996 Rydberg-atom–ion collision: classical theory of intrashell transitions *J. Phys. B: At. Mol. Opt. Phys.* **29** 3651–72

[6] Kazansky A K and Ostrovsky V N 1996 Rydberg atom–ion collisions: quantum theory of intrashell transitions *Phys. Rev. Lett.* **77** 3094

[7] Vrinceanu D and Flannery M R 2000 Classical Stark mixing at ultralow collision energies *Phys. Rev. Lett.* **85** 4880–3

[8] Vrinceanu D and Flannery M R 2000 Quantal Stark mixing at ultralow collision energies *J. Phys. B: At. Mol. Opt. Phys.* **33** L721–8

[9] Vrinceanu D and Flannery M R 2001 Analytical quantal collisional Stark mixing probabilities *J. Phys. B: At. Mol. Opt. Phys.* **34** L1–8

[10] Vrinceanu D, Onofrio R and Sadeghpour H R 2012 Angular momentum changing transitions in proton-Rydberg hydrogen atom collisions *Astrophys. J.* **747** 56

[11] Guzmán F, Badnell N R, Williams R J R, van Hoof P A M, Chatzikos M and Ferland G J 2016 H, He-like recombination spectra—I. *l*-changing collisions for hydrogen *Mon. Not. R. Astron. Soc.* **459** 3498–504

[12] Guzmán F, Badnell N R, Williams R J R, van Hoof P A M, Chatzikos M and Ferland G J 2017 H-, He-like recombination spectra—II. *l*-changing collisions for He Rydberg states *Mon. Not. R. Astron. Soc.* **464** 312–20

[13] Becker R L and MacKellar A D 1984 Theoretical initial *l* dependence of ion–Rydberg-atom collision cross sections *J. Phys. B: At. Mol. Phys.* **17** 3923–42

[14] LeVeque R J 2002 *Finite Volume Methods for Hyperbolic Problems* vol 31 (Cambridge: Cambridge University Press)
[15] Landau D P and Binder K 2014 *A Guide to Monte Carlo Simulations in Statistical Physics* (Cambridge: Cambridge University Press)
[16] Lynden-Bell D 1967 Statistical mechanics of violent relaxation in stellar systems *Mon. Not. R. Astron. Soc.* **136** 101
[17] Pengelly R M and Seaton M J 1964 Recombination spectra, II *Mon. Not. R. Astron. Soc.* **127** 165
[18] Spitzer L 1987 *Dynamical Evolution of Globular Clusters* (Princeton, NJ: Princeton University Press)
[19] Melrose D B 1989 *Instabilities in Space and Laboratory Plasmas* (Cambridge: Cambridge University Press)